agronomy

MDPI

Article

Hybrid Genome Reanalysis of Bacteriophage XaF13 Infecting *Xanthomonas vesicatoria* Provides Insights into Its Phylogenetic Relationships Within the Family *Inoviridae*

Guillermo Alejandro Solís-Sánchez [1], Evangelina Esmeralda Quiñones-Aguilar [1,*], Alexis Felipe Avalos-Salgado [1,2], Rubén Antonio Olivares-Terrones [1], Marcela Ríos-Sandoval [1] and Gabriel Rincón-Enríquez [1,*]

[1] Laboratorio de Fitopatología, Biotecnología Vegetal, Centro de Investigación y Asistencia en Tecnología y Diseño del Estado de Jalisco, A.C. Subsede Zapopan, Camino Arenero 1227, El Bajío del Arenal, Zapopan 45019, Jalisco, Mexico; gsolis_pos@ciatej.edu.mx (G.A.S.-S.); alexis.avalos@academicos.udg.mx (A.F.A.-S.); ruolivares_al@ciatej.edu.mx (R.A.O.-T.); marios_pos@ciatej.edu.mx (M.R.-S.)

[2] Departamento de Farmacobiología, Centro Universitario de Ciencias Exactas e Ingenierías (CUCEI), Universidad de Guadalajara, Guadalajara 44430, Jalisco, Mexico

* Correspondence: equinones@ciatej.mx (E.E.Q.-A.); grincon@ciatej.mx (G.R.-E.)

Abstract

Bacteriophages infecting phytopathogenic bacteria represent promising alternatives for plant disease control; however, some groups, such as filamentous bacteriophages, remain comparatively underexplored. In this study, we present a comprehensive characterization of XaF13, a filamentous bacteriophage that infects *Xanthomonas vesicatoria*, the causal agent of bacterial spot disease in pepper. Morphological analysis revealed a flexible filamentous virion architecture consistent with members of the family *Inoviridae*. To refine its genomic features, the XaF13 genome was resequenced through a hybrid approach combining newly generated Oxford Nanopore long reads with previously available Illumina data, resulting in a revised genome of 6965 bp. Comparative genomic analysis and intergenomic similarity assessment revealed low nucleotide identity with related inoviruses, supporting the recognition of XaF13 as a putative novel species based on VIRIDIC species-level thresholds. Phylogenetic reconstruction based on the Zot-like protein placed XaF13 within a broader inovirus lineage and showed that it forms a distinct evolutionary branch. In addition, physicochemical assays revealed that XaF13 remains stable across a broad pH range and tolerates brief exposure to elevated temperatures, whereas chloroform treatment and UV-C radiation reduced viral infectivity over time. Overall, these findings highlight the genomic distinctiveness and in vitro physicochemical stability of XaF13, contribute to a better understanding of filamentous bacteriophage diversity and provide a basis for future studies on its ecological role and possible interactions with phytopathogenic bacteria.

Keywords: bacteriophages; *Inovirus*; *Xanthomonas vesicatoria*; bacterial spot disease; phage therapy

Check for updates

Academic Editor: Francesco Calzarano

Received: 5 May 2026
Revised: 27 May 2026
Accepted: 29 May 2026
Published: 31 May 2026

Copyright: © 2026 by the authors. Licensee MDPI, Basel, Switzerland. This article is an open access article distributed under the terms and conditions of the Creative Commons Attribution (CC BY) license.

1. Introduction

Bacteriophages are the most widely distributed biological entities on Earth. In nature, bacteriophages play a significant role in shaping bacterial communities by modulating their populations and introducing new traits. In recent years, there has been growing interest

in bacteriophages due to their biotechnological potential across a wide range of applications, including advanced bacteriophage engineering and synthetic biology, therapeutic strategies, and clinical applications [1–3]. However, despite this progress, many aspects of bacteriophage biology remain poorly understood, particularly those related to their biological characteristics and ecological roles. In this context, filamentous bacteriophages represent an underexplored group, especially those infecting phytopathogenic bacteria.

Because of their vast diversity, no single classification system can fully capture their biological complexity. Instead, multiple complementary approaches, such as morphology, infection cycle, taxonomy, and genomic features, are used to classify and compare bacteriophages, allowing researchers to infer potential characteristics based on previously described viruses. The rapid expansion of metagenomic data has further increased the number of known bacteriophage sequences, highlighting both the limitations of current classification systems and the need for integrative frameworks to better understand bacteriophage diversity [4].

According to the most recent taxonomy established by the International Committee on Taxonomy of Viruses (ICTV) [5], filamentous bacteriophages are classified within the order *Tubulavirales*, which comprises three families: *Inoviridae*, *Paulinoviridae*, and *Plectroviridae*. Despite the increasing number of inovirus sequences identified, only a limited number of members of the family *Inoviridae* have been formally classified by the ICTV, highlighting the largely underexplored diversity of filamentous bacteriophages. Currently, this family includes more than 100 described bacteriophages infecting a wide range of bacterial hosts, including several phytopathogenic species such as *Ralstonia solanacearum*, *Ralstonia pickettii*, *Spiroplasma citri*, and various *Xanthomonas* spp. [6]. To date, only approximately thirteen filamentous bacteriophages have been reported to infect bacteria of the genus *Xanthomonas*, underscoring the limited characterization of inoviruses within this group.

Inoviruses possess circular single-stranded DNA (ssDNA) genomes enclosed within a cylindrical protein capsid. These virions lack lipid components, and their length is related to genome size. Structurally, inoviruses are characterized by flexible, filamentous particles resembling long, thin filaments [7–9]. A defining feature of inoviruses is their ability to establish chronic non-lytic infections, allowing infected bacteria to continue growing and dividing. This infection strategy enables bacteriophage propagation with limited detrimental effects on host viability, although inovirus infection may still influence host physiology, colony morphology, biofilm formation, and, in some cases, pathogenicity [10].

Moreover, the high host specificity of bacteriophages initially attracted interest in the use of bacteriophages for controlling bacterial pathogens prior to the antibiotic era [11]. Currently, bacteriophage-based approaches are increasingly recognized as valuable alternatives to conventional antimicrobial strategies in medicine, veterinary applications, and agriculture. In addition, host specificity is a key advantage of bacteriophages which minimize off-target effects, such as disruption of beneficial microbiota [1,2,12,13].

In agriculture, the use of bacteriophages for disease control represents a rapidly expanding area of plant protection, with the potential to complement or partially replace conventional chemical treatments [14–16]. Although some bacteriophage-based products have reached commercial use, including AgriPhage for bacterial spot and speck of tomato and pepper, Erwiphage for fire blight, XylPhi-PD for Pierce's disease of grapevine, and Biolyse PB for potato soft-rot management, these examples remain restricted to specific crop–pathogen systems and geographic regions [17]. Moreover, the effectiveness of bacteriophage-based strategies under field conditions depends largely on environmental stability. Factors such as temperature fluctuations, rainfall, desiccation, and solar radiation, particularly ultraviolet (UV) light, can significantly reduce bacteriophage viability on plant surfaces [18–20].

Therefore, evaluating bacteriophage tolerance to environmental stresses is an important preliminary step in assessing their practical application. Against this background, further characterization of bacteriophage XaF13 is required to refine our understanding of its genomic architecture and biological properties. In this context, the present study evaluates the basic in vitro physicochemical stability of XaF13 under controlled pH, temperature, UV-C radiation, and chloroform exposure conditions.

Although the genome of XaF13 was previously reported, advances in sequencing technologies provide an opportunity to improve genome resolution and reassess its genetic organization. In this study, we performed hybrid resequencing of the XaF13 genome, followed by comparative genomic and phylogenetic analyses to evaluate its evolutionary placement within filamentous bacteriophages. In addition, we investigated the stability of XaF13 under different physicochemical conditions, including pH, temperature, and ultraviolet (UV) radiation, to better understand its environmental resilience. The novelty of this study lies in the hybrid genome reanalysis of XaF13, the correction of its genome structure, the revised annotation of a complete Zot-like protein, and the integrated comparative placement of this bacteriophage within the family *Inoviridae*. Together, these approaches provide a refined framework for reassessing the genomic features, taxonomic position, and biological properties of XaF13.

2. Materials and Methods

2.1. Propagation and Purification of Bacteriophage XaF13

The isolation of XaF13 was previously described from soil samples collected in Yurécuaro, Michoacán, México [21]. For subsequent experiments, XaF13 was propagated in NYG broth (5 g L^{-1} peptone, 3 g L^{-1} yeast extract, 20 g L^{-1} glycerol) inoculated with *Xanthomonas vesicatoria* (laboratory strain BV865) and incubated at 28 °C for 24 h. Cellular debris was removed by centrifugation at 9000× *g* for 10 min at 4 °C, performed twice (F15-6 × 100y rotor, Thermo Scientific, Langenselbold, Germany). Next, the supernatant was filtered through a 0.22 µm polyethersulfone membrane (Merck-Millipore, Tullagreen, Ireland) to obtain a bacteriophage-containing filtrate.

Bacteriophage particles were concentrated by adding polyethylene glycol 8000 (PEG 8000) to a final concentration of 5% (*w*/*v*) and NaCl to 0.25 M, followed by overnight incubation at 4 °C. Bacteriophages were then recovered by centrifugation at 16,000× *g* for 20 min at 4 °C employing an RC5 rotor (Thermo Scientific, Pittsburgh, PA, USA) [22]. The resulting pellets were resuspended in 5 mL SM buffer, containing 50 mM Tris–HCl (pH 7.5) 100 mM NaCl, and 50 mM $MgSO_4$. This mixture was loaded onto a cesium chloride gradient (density range of 1.3 to 1.7 g mL^{-1}) and centrifuged at 100,000× *g* for 18 h at 4 °C using the AH-627/36 rotor (Thermo Scientific—Sorvall, MA, USA) to obtain pure bacteriophages. The recovered bacteriophages were dialyzed three times against SM buffer utilizing a membrane with a molecular weight cutoff of 10,000 (Spectra/Pore, Spectrum Laboratories, Rancho Dominguez, CA, USA).

2.2. Transmission Electron Microscopy

Morphological analysis was performed by placing 2 µL of purified bacteriophage XaF13 suspension (≥1 × 10^8 PFU mL^{-1}) onto a Formvar–carbon-coated grid (EMS, Hatfield, PA, USA) for 2 min. Negative staining was then performed by applying 5 µL of 2% uranyl acetate for an additional 2 min. The morphology of the purified XaF13 bacteriophage was examined using a Morgagni M-268 transmission electron microscope (FEI/PHILIPS, Eindhoven, The Netherlands).

2.3. Sensitivity of XaF13 to Physicochemical Conditions

Bacteriophage XaF13 was evaluated under various physicochemical conditions including temperature, pH, chloroform exposure, and UV (UV-C) radiation. To assess the thermal stability, a 400 µL aliquot of the bacteriophage suspension (1×10^8 PFU mL^{-1}) was incubated in a water bath at 28, 60, 70 and 80 °C for 5 min, followed by cooling to room temperature.

For pH, 50 µL of bacteriophage suspension (1×10^8 PFU mL^{-1}) was combined with 400 µL of distilled water that had been adjusted to pH levels of 2, 4, 6, 8, 10, 12, and 14 using HCl and NaOH and incubated at 28 °C for 24 h.

In the chloroform assay, 100 µL of XaF13 suspension was combined with 20 µL of chloroform and incubated at 28 °C for 24 h.

To evaluate UV sensitivity, 3 mL of bacteriophage suspension was continuously exposed to UV-C radiation at 254 nm for 90 min in a 12-well plate with a Crosslinker (UVP, Upland, CA, USA). Aliquots were collected every 30 min during exposure. Bacteriophage ØXaF18, which infects *Xanthomonas vesicatoria*, was used as a control in the chloroform susceptibility assays [23]. Bacteriophage titers were determined by performing a double-layer agar assay with soft agar. All experiments were performed in triplicate.

The detection limit of the double-layer agar assay was calculated based on the lowest dilution evaluated (10^{-2}), the plated volume of 10 µL, and two detectable plaques as the minimum observed count, resulting in a practical detection limit of 2×10^4 PFU mL^{-1}.

Data were analyzed by analysis of variance (ANOVA) when assumptions of normality and homoscedasticity were met, followed by Tukey's test for multiple comparisons ($p \leq 0.05$), using Statgraphics Centurion XVI v16.2.04 (Statgraphics Technologies, Inc., The Plains, VA, USA). When these assumptions were not met, a non-parametric Kruskal–Wallis test followed by a multiple comparison test ($p \leq 0.05$) was performed using InfoStat v2008 [24].

It should be noted that the stability assays were performed using XaF13 in aqueous suspension under controlled in vitro conditions. These assays were designed to evaluate the basic physicochemical stability of the bacteriophage in a standardized laboratory system and were not intended to assess its persistence outside suspension, on plant surfaces, or under greenhouse or field conditions.

2.4. PCR Assay

To assess the accuracy of the genome sequence of bacteriophage XaF13 previously reported [21], a polymerase chain reaction (PCR) assay was carried out. Specific primers were designed with Primer-BLAST (NCBI). The PCR mixture contained 1× high-fidelity PCR buffer (15 mM $MgCl_2$), 0.2 mM of each dNTP, and 0.1 µM of each primer (F13-01F: 5′-TCTT GCC CTC AGG CGT AAA G-3′; F13-03R: 5′-CGA TCA ATC CAC GCA CGA AC-3′; F13-04F: 5′-GCA TGC CGA AGG CCA TTT AC-3′; F13-04R: 5′-CCT ACC GGT CGC TTT AGG TC-3′).

The reaction also included 0.5 µg of template DNA and 0.5 U of high-fidelity DNA polymerase (Thermo Fisher Scientific, San Francisco, CA, USA), with nuclease-free water added to a final volume of 50 µL. PCR amplification was performed using a C1000 thermal cycler (Bio-Rad, CA, USA). The amplification conditions were as follows: initial denaturation at 94 °C for 3 min, followed by 35 cycles of denaturation at 94 °C for 30 s, annealing at 60 °C for 30 s, and extension at 68 °C for 8 min 30 s, followed by a final extension at 68 °C for 10 min.

To verify repeated sequences, an additional PCR assay was performed using a new set of primers designed with Primer-BLAST, one forward primer, XaF13-8-f 5′-CAC GAT CAA GCC GCG TAT TC-3′ and three reverse primers, XaF13-R-4_rv (5′-ACA TGC AGA TCA

GCA TCG GA-3′), XaF13-R-6_rv (5′-GTT CTC ACG CCG TTC GCG-3′), and XaF13-R-5_rv (5′-GCC GCT GCT GGT CAT GTC-3′), under the same reaction conditions, with extension at 68 °C for 30 s.

2.5. Bacteriophage DNA Extraction and Sequencing

DNA was extracted from purified XaF13 particles (>10^8 PFU mL^{-1}) with a phage-DNA extraction kit (Norgen-Biotek, ON, Canada) following the manufacturer's instructions. The genome was subsequently sequenced by the Oxford Nanopore Technologies platform (ONT, Oxford, UK). Libraries were prepared with SQK-RBK114.24 kit (Oxford, UK) and sequenced on a MinION device (Oxford, UK) using the R10.4.1 flow cell, (ONT).

Basecalling was conducted with Dorado v0.8.3 (ONT, Oxford, UK) applying duplex model dna_r10.4.1_e8.2_400bps_sup@v5.0.0. Adapter trimming and read preprocessing were carried out with Porechop ver. 0.2.4 [25]. De novo genome assembly was performed with Flye v2.9.6 [26] with default parameters.

In addition, a hybrid assembly was generated using SPAdes v4.3.0 [27,28] and the careful option, incorporating previously published Illumina reads available in the GenBank database under accession number SRX6866382. A consensus genome was constructed by aligning the sequencing reads and assemblies using Minimap2 ver. 2.30 [29], and the final consensus sequence was generated via UGENE software ver. 53.0 [30].

2.6. Phylogenetic Analysis and Genome Comparison

Comparative genomic analysis was performed to assess the relatedness of bacteriophage XaF13 to other members of the family *Inoviridae*. Pairwise intergenomic similarities were calculated using the VIRIDIC web server [31], following the recommended parameters for prokaryotic viruses. Sequences of 71 reference inovirus genomes were retrieved from the NCBI database and analyzed together with XaF13, resulting in a dataset of 72 genomes. The resulting similarity matrix was used to generate a heatmap representing pairwise nucleotide identity values among the analyzed genomes. Default VIRIDIC settings were applied, including BLASTN-based comparisons and length-normalized similarity calculations. Heatmap visualization and clustering were performed using the output provided by VIRIDIC. Intergenomic similarity thresholds for species and genus demarcation were interpreted in accordance with current guidelines of the ICTV.

Additionally, phylogenetic analysis of bacteriophage XaF13 was performed using the translated DNA sequence of ORF06 (Zot-like protein). This sequence was compared with 65 homologous sequences from bacteriophages belonging to the family *Inoviridae*. Sequence alignment was performed using the MUSCLE algorithm, and phylogenetic reconstruction was conducted using the Neighbor-Joining (NJ) method; both analyses were implemented in MEGA software v12 [32]. Evolutionary distances were computed using the Poisson amino acid substitution model and are expressed as the number of amino acid substitutions per site. Rate variation among sites was modeled using a gamma distribution ($\gamma = 2.00$), and the pattern among lineages was assumed to be homogeneous. Branch support was assessed using the bootstrap method with 1000 replicates. Gaps and missing data were treated using partial deletion, with a site coverage cutoff of 95%.

Comparative genomic analyses were performed using Easyfig v2.2.5 [33] to visualize sequence similarity and gene synteny among bacteriophage genomes. Genome sequences were imported in FASTA and GenBank formats, and pairwise comparisons were conducted using BLAST+ (bastn) ver. 2.17.0. Default parameters were applied, with sequence similarity thresholds adjusted to optimize visualization.

3. Results

3.1. Morphology

The *Xanthomonas vesicatoria* bacteriophage XaF13 was isolated from soil samples collected from pepper crops affected by bacterial spot disease. In double-layer plaque assays, XaF13 produced clear plaques of approximately 1 mm in diameter (Figure 1), indicative of active infection and efficient propagation under the tested conditions.

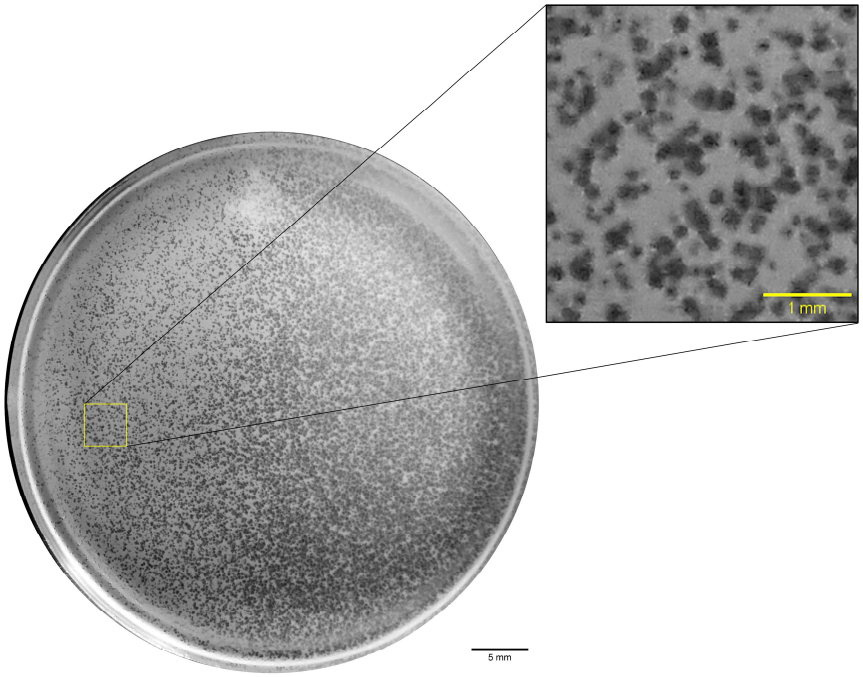
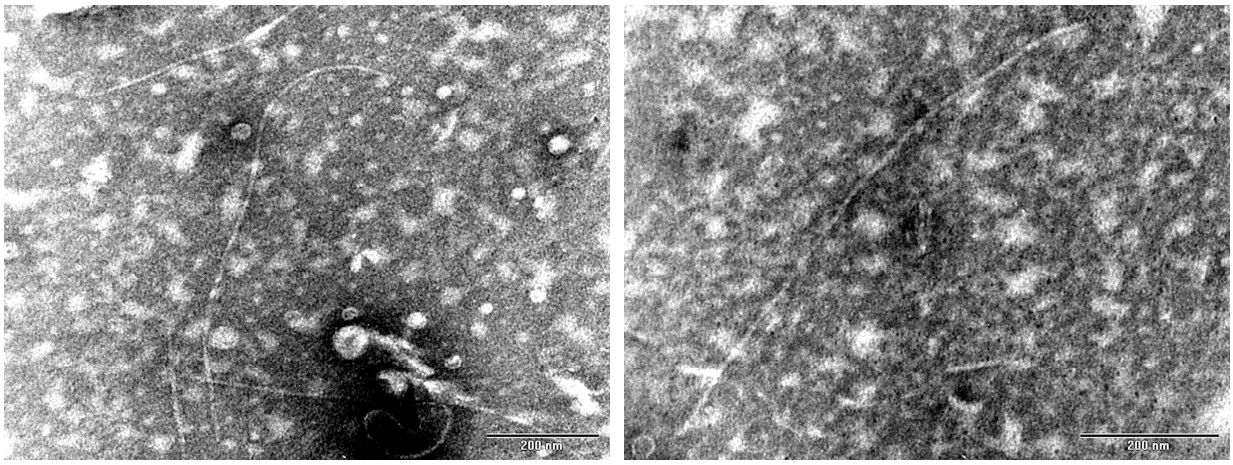


Figure 1. Plaque morphology of bacteriophage XaF13 on *Xanthomonas vesicatoria*. Plaques were obtained using a double-layer agar assay and appeared as numerous small, clear plaques distributed across the bacterial lawn. The inset highlights a magnified region of the plate, illustrating plaque morphology in detail. Plaque diameters were typically <1 mm. Samples were plated on 90 mm Petri dishes. Scale bars: 5 mm (main image) and 1 mm (inset).

Transmission electron microscopy (TEM) analysis revealed that XaF13 exhibits a flexible filamentous morphology, with an average length of 850 nm (±13 nm) and a width of approximately 8.5 nm (n = 8) (Figure 2). These structural features are consistent with filamentous bacteriophages, including members of the order *Tubulavirales* [5]. In addition, genomic features and comparative genomic analyses further support the placement of XaF13 within filamentous inoviruses, since morphology alone is insufficient for formal ICTV classification.

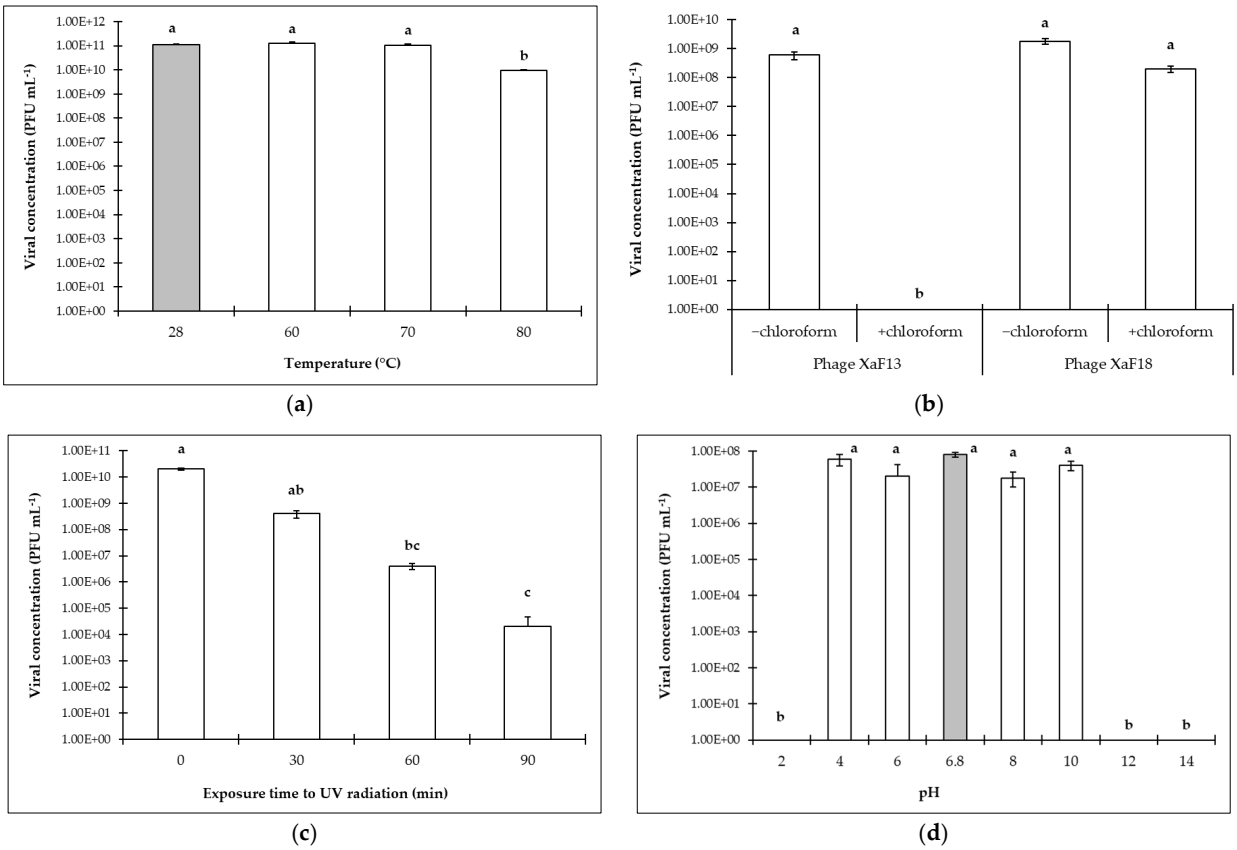
3.2. Sensitivity to Physicochemical Conditions

Temperature stability assays showed that XaF13 remained detectable after 5 min of exposure to elevated temperatures. Viral titers were 1.13 (±0.12) × 10^{11} PFU mL^{-1} at 28 °C, 1.27 (±0.31) × 10^{11} PFU mL^{-1} at 60 °C, 1.07 (±0.23) × 10^{11} PFU mL^{-1} at 70 °C, and 9.33 (±1.15) × 10^{9} PFU mL^{-1} at 80 °C. Thus, XaF13 remained detectable at 80 °C, although the titer decreased by approximately 1.1 $\log_{10}$ relative to the 28 °C control (Figure 3a).



(**a**) (**b**)

Figure 2. Transmission electron micrographs of bacteriophage XaF13 isolated from soil samples. Negatively stained particles (2% uranyl acetate) show filamentous virions with a length of ~850 nm, consistent with members of the *Inoviridae* family. (**a**) Multiple phage particles; (**b**) single phage particle. Magnification: 89,000× (**a**); 110,000× (**b**).



(**a**) (**b**)

(**c**) (**d**)

Figure 3. Stability and infectivity of bacteriophage XaF13 under different physicochemical treatments. XaF13 was exposed to different temperatures for 5 min (**a**), chloroform treatment for 24 h (**b**), UV-C radiation at 254 nm for different exposure times (**c**), and different pH conditions for 24 h (**d**). In panel (**b**), the response of XaF13 to chloroform is compared with that of phage ØXaF18 under untreated conditions (−chloroform) and chloroform-treated conditions (+chloroform). Gray bars indicate the control conditions used as references for XaF13 viability under *in vitro* conditions. Bars represent the mean ± standard error. Different lowercase letters within each graph indicate significant differences according to Tukey's test (**a**) or the Kruskal–Wallis test (**b**–**d**), with a significance level of 5% ($p \leq 0.05$).

After chloroform exposure, infectious XaF13 particles were not detected, with titers falling below the assay detection limit, whereas the untreated XaF13 control showed a titer of 6.67 (±3.06) × 10^8 PFU mL^{-1}. In contrast, bacteriophage ØXaF18 decreased from 1.53 (±0.64) × 10^9 PFU mL^{-1} in the untreated control to 1.53 (±0.81) × 10^8 PFU mL^{-1} after chloroform treatment, corresponding to an approximately 1.0 $\log_{10}$ reduction (Figure 3b).

Under UV-C exposure, XaF13 titers decreased progressively from 1.87 (±0.23) × 10^{10} PFU mL^{-1} at 0 min to 3.07 (±2.16) × 10^8 PFU mL^{-1} at 30 min, 4.07 (±1.90) × 10^6 PFU mL^{-1} at 60 min, and 4.67 (±4.62) × 10^4 PFU mL^{-1} at 90 min. This corresponds to an approximately 5.6 $\log_{10}$ reduction after 90 min of UV-C irradiation (Figure 3c).

For pH stability, XaF13 remained detectable after exposure to pH 4–10, with titers of 5.00 (±3.61) × 10^7 PFU mL^{-1} at pH 4, 3.73 (±3.72) × 10^7 PFU mL^{-1} at pH 6, 2.47 (±1.33) × 10^7 PFU mL^{-1} at pH 8, and 4 (±2) × 10^7 PFU mL^{-1} at pH 10, compared with 8.00 (±2) × 10^7 PFU mL^{-1} in the pH 7 control. In contrast, no infectious particles were detected at pH 2, pH 12, or pH 14, with titers below the assay detection limit of 2 × 10^{-4} PFU mL^{-1} (Figure 3d).

3.3. Genomic Characterization and Comparative Analysis of Bacteriophage XaF13

3.3.1. Validation and Reassembly of the XaF13 Genome

The original 7045 bp genome structure of bacteriophage XaF13 was initially validated by PCR amplification of two overlapping regions of 5337 bp and 6798 bp, consistent with in silico predictions (Supplementary Figure S1). However, further genome inspection revealed the presence of an 80 bp tandem repeat at the end of ORF06 (Zot-like protein) (Supplementary Figure S2). Additional PCR assays were performed to verify this feature, confirming that only a single copy of the sequence is present (Figure 4).

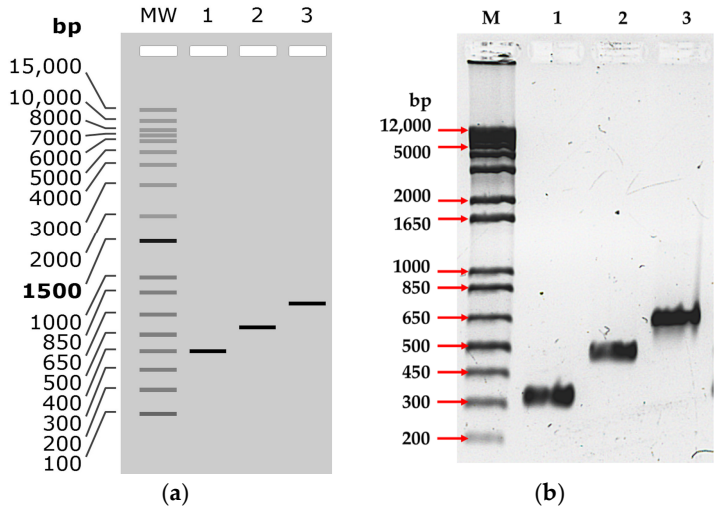


Figure 4. Experimental validation of repeated sequences in the XaF13 genome. (**a**) In silico agarose gel electrophoresis showing the predicted amplicon sizes within the 7045 bp XaF13 genome. Lane MW, molecular weight marker, 1 Kb+ (Invitrogen, VL, LT); lane 1, primers XaF13-8-f/XaF13-R-4_rv (400 bp); lane 2, primers XaF13-8-f/XaF13-R-6_rv (558 bp); lane 3, primers XaF13-8-f/XaF13-R-5_rv (739 bp). (**b**) Agarose gel electrophoresis (1.2%) of PCR products showing amplicons of lower molecular weight than those predicted in silico. Lane M, molecular weight marker, 1 Kb+ (Invitrogen, VL, LT); lanes 1–3 correspond to the same primer combinations as: lane 1, primers XaF13-8-f/XaF13-R-4_rv (400 − 80 = 320 bp); lane 2, primers XaF13-8-f/XaF13-R-6_rv (558 − 80 = 478 bp); lane 3, primers XaF13-8-f/XaF13-R-5_rv (739 − 80 = 659 bp).

Therefore, the XaF13 genome was resequenced using third-generation Oxford Nanopore Technologies (ONT), followed by hybrid assembly with previously generated Il-

lumina data. ONT sequencing produced 2142 reads, with an approximate coverage of 411x. Hybrid assembly combining ONT and Illumina data yielded a 6965 bp consensus sequence.

This assembly differed from the previously reported genome by 80 bp, resulting in a revised genome organization. Specifically, ORF6 and ORF7 were merged into a single open reading frame (ORF6), which exhibited high similarity and full-length coverage to Zot-like proteins in the NCBI database. Additionally, the coordinates of upstream ORFs were adjusted, reducing the total number of predicted ORFs from 14 to 13. Further functional analysis by BLASTp confirmed the function of all ORFs except ORF 13 (formerly ORF14) which was reannotated as a hypothetical protein rather than a DNA polymerase, as previously reported (Figure 5).

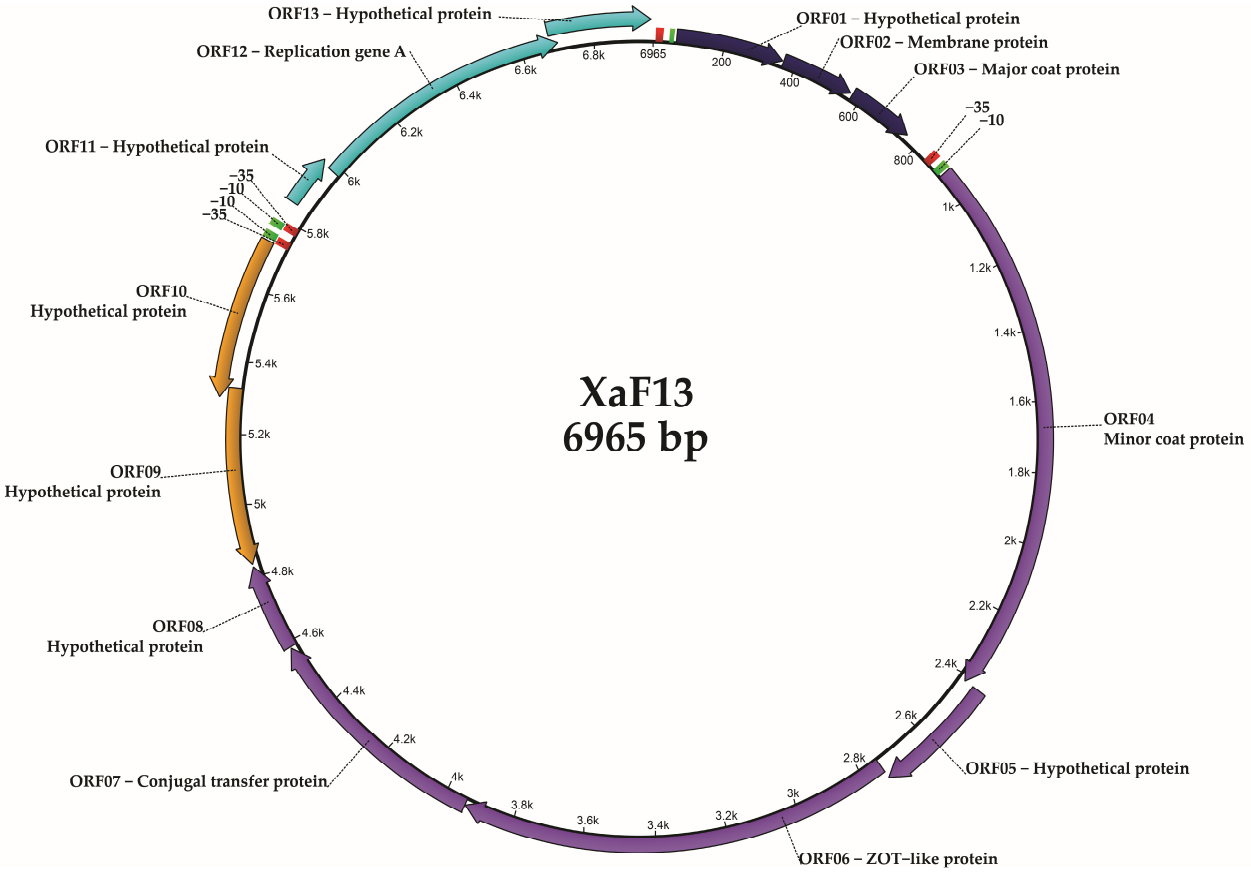


Figure 5. Updated genetic map of bacteriophage XaF13. The genome start site was arbitrarily assigned to ORF1. Arrows indicate predicted open reading frames and their transcriptional direction, while thin arrows denote predicted promoter positions and orientations.

The genome sequence of bacteriophage XaF13 is available in GenBank under accession number MN335248.1, with the corresponding RefSeq record as NC_062737.1. The Illumina raw sequence reads are available in the Sequence Read Archive (SRA) under accession number SRX6866382, and the ONT reads are available under accession number SRR38084410, associated with BioProject PRJNA566170. The corrected genome sequence generated using a hybrid Illumina–ONT assembly approach is available under GenBank accession number MN335248.2, whereas the corresponding RefSeq record is expected to be updated accordingly.

3.3.2. Comparative Genomic Analysis of Bacteriophage XaF13 and Related Inoviruses

To assess the genomic relatedness of bacteriophage XaF13 to other filamentous bacteriophages, pairwise intergenomic similarities were calculated using the VIRIDIC web

tool. The analysis included 71 inovirus genomes together XaF13 infecting diverse bacterial hosts. The resulting heatmap revealed several distinct clusters corresponding to bacteriophages infecting related hosts. Bacteriophage XaF13 grouped with inoviruses infecting *Xanthomonas* species, suggesting a shared evolutionary origin within this lineage of filamentous bacteriophages (Figure 6, Supplementary Figure S3).

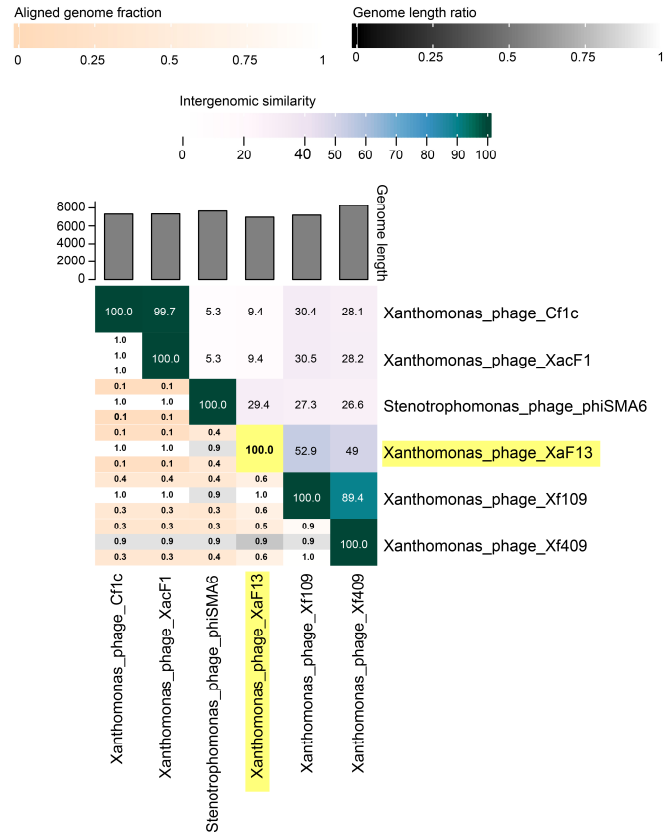


Figure 6. Intergenomic similarity among filamentous bacteriophages calculated using VIRIDIC. The heatmap shows pairwise nucleotide similarities between complete viral genomes. Bacteriophages infecting related bacterial hosts tend to cluster together. XaF13, highlighted in yellow, clusters within the clade of inoviruses infecting *Xanthomonas* species but shows relatively low similarity values (<60%) to its closest relatives. The complete heatmap whit the remaining 66 inovirus sequences (72 sequences in total) is provided in Supplementary Figure S3.

Despite this clustering, the overall nucleotide similarity between XaF13 and previously described *Xanthomonas* inoviruses was relatively low. The highest intergenomic similarity was observed with *Xanthomonas* bacteriophage Xf109 (52.7%) and *Xanthomonas* bacteriophage Xf409 (48.8%), followed by *Stenotrophomonas* bacteriophage ØSMA6 (29.3%). In contrast, markedly lower values (<10%) were observed with *Xanthomonas* bacteriophages XacF1 and Cf1c, as well as *Stenotrophomonas* bacteriophage PSH1. These values are well below the 95% similarity threshold recommended by the ICTV for viral species demarcation.

In agreement with these findings, phylogenetic analysis of the Zot-like protein encoded by ORF6 of bacteriophage XaF13 revealed that its clusters within a well-supported clade of bacteriophages belonging to the family *Inoviridae*. The XaF13 sequence grouped closely with Zot-like proteins from related filamentous bacteriophages infecting Gram-negative bacteria, indicating a conserved evolutionary origin among bacteriophage-associated Zot proteins (Figure 7). Notably, this clade was clearly separated from canonical Zot proteins described in *Vibrio cholerae*.

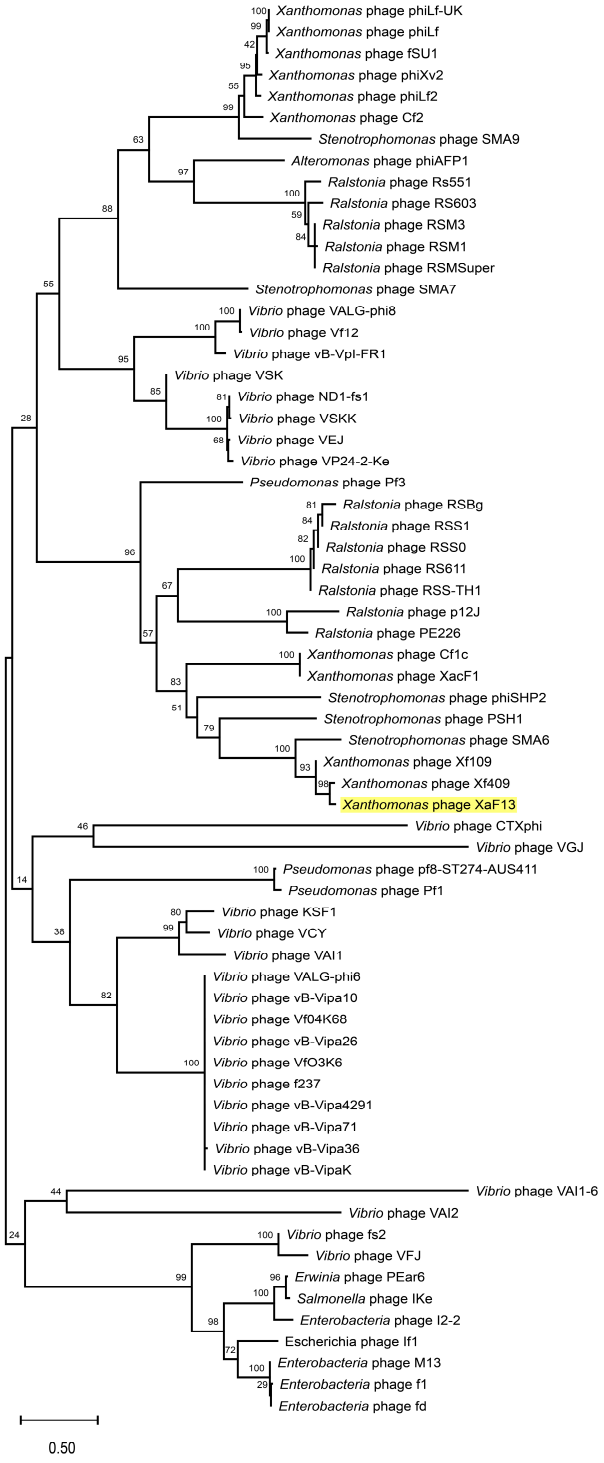


Figure 7. Phylogenetic analysis of Zot proteins showing the position of bacteriophage XaF13 among filamentous bacteriophages. XaF13, highlighted in yellow, forms a distinct cluster within the *Inoviridae* lineage, suggesting evolutionary divergence from closely related phages. The tree was inferred using the Neighbor-Joining (NJ) method from MUSCLE-aligned amino acid sequences. Evolutionary distances were computed using the Poisson amino acid substitution model with gamma-distributed rates among sites ($\gamma = 2.00$). Branch support was assessed using 1000 bootstrap replicates. The scale bar indicates amino acid substitutions per site.

3.3.3. Comparative Genomics of XaF13 with Xf109 and ØSMA6

Comparative genomic analysis revealed a conserved genomic organization among XaF13 and related filamentous bacteriophages infecting *Xanthomonas* species. Extensive

regions of synteny were observed, particularly across modules associated with replication, structural proteins, and the Zot-like protein, supporting a shared evolutionary origin (Figure 8). The Zot-like protein region showed strong conservation between XaF13 and Xf109, consistent with phylogenetic analysis.

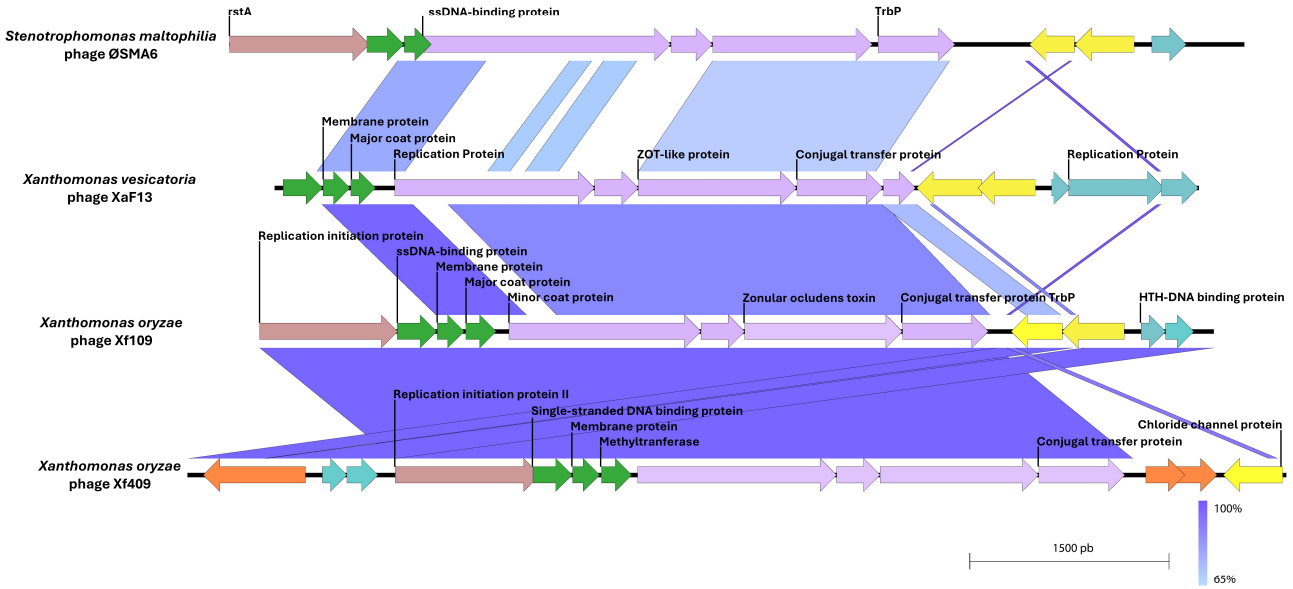


Figure 8. Comparative genomic organization of bacteriophage XaF13 and related filamentous bacteriophages. Genomes of XaF13 and related filamentous bacteriophages infecting Xanthomonas spp. and Stenotrophomonas maltophilia are shown. Predicted open reading frames (ORFs) are represented as arrows indicating transcriptional direction, with annotated functions. Shaded regions between genomes indicate sequence similarity (65–100% identity), with color intensity proportional to the level of identity. Conserved modules, including replication, structural proteins, and conjugative transfer are evident across the analyzed genomes. The figure was generated with Easyfig v2.2.5. Scale bar indicates genome length (bp).

In contrast, bacteriophage Xf409 exhibited greater divergence, particularly in terminal regions, including the presence of additional genes such as methyltransferases and hypothetical proteins, suggesting genome plasticity and potential horizontal gene transfer events. The more distantly related bacteriophage ØSMA6 displayed limited similarity, restricted to conserved core regions. Overall, these results highlight the modular genome architecture of filamentous bacteriophages and support the classification of XaF13 within a distinct yet conserved lineage associated with *Xanthomonas* hosts.

4. Discussion

The distinct genomic features and low intergenomic similarity observed for XaF13 relative to previously described bacteriophages support its classification as a novel member of the family *Inoviridae* and reinforce the idea that the diversity of filamentous bacteriophages infecting phytopathogenic bacteria remains substantially underestimated.

Transmission electron microscopy (TEM) of bacteriophage XaF13 revealed a filamentous morphology with a flexible virion architecture, consistent with its placement within the family *Inoviridae*, order *Tubulavirales*. Viral classification has traditionally relied, in part, on morphological criteria, which, although not always directly correlated with functional properties, provide a useful framework for understanding structural diversity. Most viruses described to date can be broadly categorized into three major morphological groups: icosahedral, pleomorphic and filamentous forms [34]. Among bacteriophages, tailed icosa-

hedral phages have been extensively studied, whereas filamentous bacteriophages infecting phytopathogenic bacteria remain comparatively underexplored.

The structural organization observed in XaF13 is consistent with that of inoviruses, a group generally associated with extrusion-based release mechanisms and chronic, non-lytic infections [35]. Nevertheless, these biological processes were not directly evaluated in the present study. Therefore, the possible extrusion-based release mechanism and chronic infection strategy of XaF13 should be considered putative and inferred from its structural and genomic similarity to other members of the family *Inoviridae*. Further studies will be necessary to experimentally determine the infection dynamics, release mechanism, and effects of XaF13 on host physiology.

In addition, XaF13 maintained infectivity across a wide pH range and remained detectable after short-term exposure to elevated temperatures, including 80 °C for 5 min, indicating a degree of physicochemical stability under controlled in vitro conditions. Nevertheless, this thermal tolerance should not be interpreted as evidence of adaptation to soil or plant-surface environments, since such temperatures are not representative of typical field conditions. Further studies under environmental conditions are required to determine the ecological relevance of these traits.

Exposure to UV-C radiation caused a marked reduction in XaF13 infectivity, with titers decreasing progressively over time and reaching an approximately 5.6-$\log_{10}$ reduction after 90 min under controlled in vitro conditions. This result indicates that XaF13 is susceptible to UV-C radiation, which may represent a limitation for its persistence in exposed environments and for any future field-oriented application.

Previous studies have suggested that UV sensitivity or tolerance in filamentous bacteriophages may be influenced by the protein composition and structural organization of the viral capsid, including hydrogen bonding and steric interactions within the major capsid protein [36]. However, UV-C irradiation at 254 nm does not fully mimic natural sunlight exposure, where UV-A and UV-B radiation are more relevant under field conditions.

In this regard, several strategies have been proposed to reduce bacteriophage inactivation caused by UV radiation on foliage. Various protective formulations based on natural compounds, including carrot, red pepper, and beetroot extracts, have been shown to improve bacteriophage viability after UV exposure, likely due to the light-absorbing properties of plant pigments such as carotenoids and betalains, as well as phenolic compounds. Similarly, other substances, including aromatic amino acids, soy peptone, casein, and astaxanthin, have also exhibited UV-protective effects [37].

In addition, optimized polysorbate 80-kaolin formulations have been shown to improve the UV stability and leaf adsorption of bacteriophages, supporting the importance of formulation design for phage persistence on foliage [38]. Other formulations, such as skim milk–sucrose, have also improved phage survival under both UV exposure and darkness, allowing phages to persist on leaf surfaces under greenhouse conditions [39].

The stability assays conducted in this study were performed using XaF13 in aqueous suspension under controlled in vitro conditions. In natural or greenhouse environments, bacteriophage persistence may be influenced by additional factors, including desiccation, UV-A and UV-B radiation, natural sunlight, rainfall, temperature fluctuations, leaf surface properties, and interactions with formulation components. Therefore, these results do not indicate that XaF13 is unable to survive outside a suspension, but they also cannot be directly extrapolated to plant surfaces or field environments.

These findings suggest that protective formulations, UV-protective additives, carrier-based delivery systems, and application strategies such as evening or early-morning application should be explored to reduce UV-mediated loss of XaF13 infectivity. Nevertheless,

these approaches should be validated specifically for XaF13 under UV-A/UV-B radiation, natural sunlight, and plant surfaces before any field-oriented conclusions are drawn.

Interestingly, XaF13 produces clear plaques in double-layer agar assays. Filamentous bacteriophages are typically associated with turbid plaques, reflecting chronic infections that do not necessarily result in host cell lysis. Nevertheless, clear plaque formation has been reported for several filamentous bacteriophages, including enterobacteria bacteriophages fd, f1 and M13, as well as *Xanthomonas campestris* bacteriophage Cf1t [40–43]. In many cases, infections with filamentous bacteriophages yield a mixture of turbid and clear plaques. In contrast, XaF13 consistently produced clear plaques under the conditions tested.

Clear plaque formation in filamentous bacteriophages has been associated with mutations affecting genes involved in replication and virion assembly. For example, mutations in ORFII of bacteriophage Cf1t and in the pI and pIV proteins of bacteriophage f1 have been reported to exert deleterious effects on host cells, leading to clear plaque phenotypes. In Cf1t, two classes of mutations have been described: substitutions at positions 442 and 491 and a single-base deletion at position 442, both located upstream of ORFII. These mutations are thought to influence ORFII expression, thereby affecting plaque turbidity. Similarly, expression of pI and pIV proteins in bacteriophage f1 can be toxic to the host even at low levels, contributing to clear plaque formation [42,43].

In XaF13, no homologs of ORFII, pI, or pIV were identified, suggesting that the mechanism underlying clear plaque formation differs from those described for f1 and Cf1t bacteriophages. These observations indicate that XaF13 may employ an alternative mechanism affecting host viability or bacteriophage release dynamics. However, further studies are required to elucidate the molecular basis of this phenotype.

Genome reanalysis through a hybrid sequencing approach resolved a discrepancy in the previously reported sequence. The 80 bp difference corresponded to an assembly-related error involving a repeated region, rather than to an independent annotation error or a deletion identified by the new sequencing data. Correction of this region modified the local coding structure and supported the reannotation of two previously separated ORFs as a single continuous gene encoding a Zot-like protein.

Moreover, the combined genomic and phylogenetic analyses provide a comprehensive framework for understanding the evolutionary placement of bacteriophage XaF13 within filamentous bacteriophages. Intergenomic similarity analysis through VIRIDIC revealed that XaF13 shares relatively low nucleotide identity relative to previously described inoviruses, including those infecting *Xanthomonas* spp. These values fall below the thresholds commonly used for species demarcation, supporting the classification of XaF13 as a novel species within the family *Inoviridae*. This observation is consistent with clustering patterns obtained from VIRIDIC, which did not assign XaF13 to any defined species-level group.

Phylogenetic reconstruction based on the Zot-like protein further supports this conclusion. Previous studies have demonstrated that Zot proteins are among the most conserved and phylogenetically informative markers in filamentous bacteriophages; accordingly, analyses based on these proteins provide a robust framework for their classification [10]. In this context, Zot-based phylogeny placed XaF13 within a broader inovirus lineage comprising bacteriophages infecting *Xanthomonas*, *Stenotrophomonas*, *Ralstonia*, and *Vibrio* spp. Notably, as shown in Figure 7, XaF13 clusters with phages such as Xf109 and Xf409 but forms a distinct branch, supporting its evolutionary divergence despite moderate bootstrap support in some internal nodes.

The phylogenetic placement of XaF13, together with the clear distinction between bacteriophage-associated Zot-like proteins and canonical bacterial Zot-like proteins, suggests that these proteins constitute a specialized evolutionary lineage [44,45]. This lineage may have been shaped by horizontal gene transfer and host-specific adaptation. From a

functional perspective, the presence of a Zot-like protein in XaF13 suggests potential roles beyond structural or replication-associated functions, possibly contributing to interactions with the bacterial host. In filamentous phages, Zot homologs have been associated with modulation of host physiology and may influence processes such as membrane permeability or virulence-related traits [10,44]. In the context of *Xanthomonas* spp., which are important phytopathogens, the acquisition or diversification of such genes may have ecological and evolutionary implications, including enhanced adaptability or fitness within plant-associated environments [46]. Given the central role of Zot proteins in virion morphogenesis, the observed divergence may also reflect structural or functional adaptations influencing bacteriophage assembly and host interaction dynamics [47–49].

Comparative genomic analysis revealed conserved genome organization among XaF13 and related filamentous bacteriophages, including Xf109, Xf409, and ØSMA6, particularly within modules associated with replication, structural proteins, and the Zot-like region. Consistent with this observation, inovirus classification increasingly relies on genomic organization rather than nucleotide or amino acid sequence homology, as bacteriophage-encoded genes and proteins are generally poorly conserved, with only a few notable exceptions [45,50]. The conservation of gene order and the high similarity observed in core functional regions support a shared evolutionary origin and highlight strong functional constraints on essential genes. In contrast, variability in certain genomic regions suggests the occurrence of horizontal gene transfer events and genome rearrangements, contributing to the plasticity of inoviruses [51].

This balance between conserved architecture and sequence divergence is consistent with the modular evolution of filamentous bacteriophages, whose compact circular genomes must preserve essential functions while allowing for genetic exchange that facilitates host adaptation [5,8]. Thus, the structural conservation observed among XaF13 and related phages does not contradict their low nucleotide similarity; rather, it reflects an evolutionary pattern in which essential modules are maintained while accessory regions diversify under selective pressures.

Together, these findings indicate that XaF13 represents a genetically distinct and evolutionarily divergent member of the family *Inoviridae*. Overall, the genomic and phylogenetic evidence supports the recognition of XaF13 as a putative novel species, pending formal taxonomic evaluation. Moreover, XaF13 appears to belong to a broader lineage of filamentous bacteriophages that includes phages infecting both *Xanthomonas* and non-*Xanthomonas* hosts, such as *Stenotrophomonas*. These results underscore the importance of integrating complementary analytical approaches to accurately resolve bacteriophage taxonomy and highlight the extensive, yet still underexplored, diversity of filamentous bacteriophages in plant-associated environments.

5. Conclusions

The *Xanthomonas vesicatoria* bacteriophage XaF13 represents a genetically distinct and evolutionarily divergent member of the family *Inoviridae*, as supported by concordant evidence from morphological, genomic, and phylogenetic analyses. Hybrid genome reanalysis resolved a previously undetected sequence discrepancy, leading to a refined genome organization and the reannotation of a complete Zot-like protein. This result highlights the importance of combining long- and short-read sequencing approaches for accurate genome reconstruction and annotation, particularly in small viral genomes containing repetitive or structurally complex regions.

The low intergenomic similarity observed between XaF13 and previously described filamentous bacteriophages, together with its distinct phylogenetic placement based on the Zot-like protein, supports the recognition of XaF13 as a putative novel species, pending

formal taxonomic evaluation. Although XaF13 is associated with *Xanthomonas*, its phylogenetic affinity to phages infecting other bacterial genera, such as *Stenotrophomonas*, suggests that related inoviruses may have diversified across different bacterial hosts. The coexistence of conserved genomic architecture and substantial sequence divergence supports a modular model of evolution in filamentous bacteriophages, in which essential functional modules are maintained while accessory regions diversify under selective pressures.

Moreover, the biological features observed for XaF13, including its plaque phenotype and stability under selected physicochemical conditions, provide useful information for understanding its biology and environmental persistence. However, the ecological and applied significance of these traits remains to be determined. The current findings are supported by genomic analyses and in vitro characterization under controlled conditions. This study did not include *in planta* disease-control assays, host-range analysis, evaluation of infection dynamics, assessment of the effect of chronic infection on host virulence, formulation stability tests, or field-relevant assays under UV-A/UV-B exposure, natural sunlight, and leaf-surface conditions. Therefore, the potential role of XaF13 in plant disease dynamics or biological disease management should be considered preliminary and requires further validation under greenhouse and field conditions. Overall, this study expands current knowledge of filamentous bacteriophage diversity associated with phytopathogenic bacteria and underscores the need for integrated genomic, phylogenetic, functional, ecological, and plant-based assays to clarify their taxonomy, evolutionary relationships, and biological relevance in plant-associated environments.

Supplementary Materials: The following supporting information can be downloaded at: https://www.mdpi.com/article/10.3390/agronomy16111090/s1, Figure S1: In silico prediction and experimental validation of bacteriophage XaF13 genomic fragments; Figure S2: Genomic location of repeated sequences (each one 80 bp) and validation primers in bacteriophage XaF13; Figure S3: Expanded VIRIDIC-based heatmap.

Author Contributions: Conceptualization, G.A.S.-S., E.E.Q.-A. and G.R.-E.; methodology, G.A.S.-S., E.E.Q.-A., M.R.-S. and G.R.-E.; software, G.A.S.-S. and R.A.O.-T.; validation, G.A.S.-S. and G.R.-E.; formal analysis, G.A.S.-S. and G.R.-E.; investigation, G.A.S.-S., R.A.O.-T., M.R.-S. and A.F.A.-S.; resources, E.E.Q.-A. and G.R.-E.; data curation, G.A.S.-S., M.R.-S. and R.A.O.-T.; writing—original draft preparation, G.A.S.-S.; writing—review and editing, G.A.S.-S., R.A.O.-T., M.R.-S., E.E.Q.-A., G.R.-E.; visualization, G.A.S.-S.; supervision, E.E.Q.-A. and G.R.-E.; project administration, E.E.Q.-A. and G.R.-E.; funding acquisition, E.E.Q.-A. and G.R.-E. All authors have read and agreed to the published version of the manuscript.

Funding: This research was funded by SECIHTI (Secretaría de Ciencia, Humanidades, Tecnología e Inovación, México), grant number APN-2015-01-338 and MADTEC-2025-M-158; and G.A.S.-S. is grateful to SECIHTI for the scholarship granted for postdoctoral studies (CVU 204332).

Data Availability Statement: The data presented in this study are available on request from the corresponding author. The data are not publicly available due to privacy.

Acknowledgments: We acknowledge the support provided to the project "*In silico* analysis of genomic sequences from microorganisms of agricultural importance" by the Data Analysis and Supercomputing Center (CADS) at the Centro Universitario de Ciencias Económico Administrativas (CUCEA) of the University of Guadalajara through access to the Leo Atrox supercomputer. During the preparation of this manuscript, the author(s) used AI tools for grammar correction, language editing, and text refinement. The authors have reviewed and edited the output and take full responsibility for the content of this publication.

Conflicts of Interest: The authors declare no conflicts of interest.

References

1. Kaneko, T.; Nakatsuka, K.; Tsuneda, S. Phage cocktails: State-of-the-art technologies and strategies for effective design. *FEMS Microbiol. Rev.* **2026**, *50*, fuaf061. [CrossRef]
2. Strathdee, S.A.; Hatfull, G.F.; Mutalik, V.K.; Schooley, R.T. Phage therapy: From biological mechanisms to future directions. *Cell* **2023**, *186*, 17–31. [CrossRef]
3. Wu, P.; Li, W.; Zhang, W.; Li, S.; Deng, B.; Xu, S.; Li, Z. Advanced strategies in phage research: Innovations, applications, and challenges. *Microorganisms* **2025**, *13*, 1960. [CrossRef]
4. Valencia-Toxqui, G.; Ramsey, J. How to introduce a new bacteriophage on the block: A short guide to phage classification. *J. Virol.* **2024**, *98*, e0182123. [CrossRef]
5. Knezevic, P.; Adriaenssens, E.M.; Siddell, S.G.; Lefkowitz, E.J.; Sabanadzovic, S.; Simmonds, P.; Zerbini, F.M.; Smith, D.B.; Orton, R.J. ICTV virus taxonomy profile: *Inoviridae*. *J. Gen. Virol.* **2021**, *102*, 001614. [CrossRef]
6. Walker, P.J.; Siddell, S.G.; Lefkowitz, E.J.; Mushegian, A.R.; Adriaenssens, E.M.; Alfenas-Zerbini, P.; Dempsey, D.M.; Dutilh, B.E.; García, M.L.; Curtis Hendrickson, R.; et al. Recent Changes to virus taxonomy ratified by the International Committee on Taxonomy of Viruses (2022). *Arch. Virol.* **2022**, *167*, 2429–2440. [CrossRef] [PubMed]
7. Marvin, D.A.; Symmons, M.F.; Straus, S.K. Structure and assembly of filamentous bacteriophages. *Prog. Biophys. Mol. Biol.* **2014**, *114*, 80–122. [CrossRef] [PubMed]
8. Rakonjac, J.; Russel, M.; Khanum, S.; Brooke, S.J.; Rajič, M. Filamentous phage: Structure and biology. In *Advances in Experimental Medicine and Biology*; Lim, T.S., Ed.; Springer New York LLC: New York, NY, USA, 2017; Volume 1053, pp. 1–20.
9. Rakonjac, J. Filamentous bacteriophages: Biology and applications. *Encycl. Life Sci.* **2012**, *13*, 51–76. [CrossRef]
10. Hay, I.D.; Lithgow, T. Filamentous phages: Masters of a microbial sharing economy. *EMBO Rep.* **2019**, *20*, EMBR201847427. [CrossRef] [PubMed]
11. Olawade, D.B.; Fapohunda, O.; Egbon, E.; Ebiesuwa, O.A.; Usman, S.O.; Faronbi, A.O.; Fidelis, S.C. Phage therapy: A targeted approach to overcoming antibiotic resistance. *Microb. Pathog.* **2024**, *197*, 107088. [CrossRef]
12. Chan, B.K.; Abedon, S.T.; Loc-Carrillo, C. Phage cocktails and the future of phage therapy. *Future Microbiol.* **2013**, *8*, 769–783. [CrossRef] [PubMed]
13. Hess, K.L.; Jewell, C.M. Phage display as a tool for vaccine and immunotherapy development. *Bioeng. Transl. Med.* **2020**, *5*, e10142. [CrossRef]
14. Balogh, B.; Jones, J.; Iriarte, F.; Momol, M. Phage therapy for plant disease control. *Curr. Pharm. Biotechnol.* **2010**, *11*, 48–57. [CrossRef]
15. Jones, J.B.; Jackson, L.E.; Balogh, B.; Obradovic, A.; Iriarte, F.B.; Momol, M.T. Bacteriophages for plant disease control. *Annu. Rev. Phytopathol.* **2007**, *45*, 245–262. [CrossRef]
16. Jones, J.B.; Svircev, A.M.; Obradović, A.Ž. Crop Use of bacteriophages. In *Bacteriophages*; Harper, D.R., Abedon, S.T., Burrowes, B.H., McConville, M.L., Eds.; Springer International Publishing: Cham, Switzerland, 2018; pp. 1–18.
17. Wagemans, J.; Holtappels, D.; Vainio, E.; Rabiey, M.; Marzachì, C.; Herrero, S.; Ravanbakhsh, M.; Tebbe, C.C.; Ogliastro, M.; Ayllón, M.A.; et al. Going viral: Virus-based biological control agents for plant protection. *Annu. Rev. Phytopathol.* **2022**, *60*, 21–42. [CrossRef] [PubMed]
18. Iriarte, F.B.; Balogh, B.; Momol, M.T.; Smith, L.M.; Wilson, M.; Jones, J.B. Factors affecting survival of bacteriophage on tomato leaf surfaces. *Appl. Environ. Microbiol.* **2007**, *73*, 1704–1711. [CrossRef]
19. Jończyk, E.; Kłak, M.; Międzybrodzki, R.; Górski, A. The influence of external factors on bacteriophages—Review. *Folia Microbiol.* **2011**, *56*, 191–200. [CrossRef] [PubMed]
20. Jones, J.B.; Vallad, G.E.; Iriarte, F.B.; Obradović, A.; Wernsing, M.H.; Jackson, L.E.; Balogh, B.; Hong, J.C.; Momol, M.T. Considerations for using bacteriophages for plant disease control. *Bacteriophage* **2012**, *2*, e23857. [CrossRef]
21. Solís-Sánchez, G.A.; Quiñones-Aguilar, E.E.; Fraire-Velázquez, S.; Vega-Arreguín, J.; Rincón-Enríquez, G. Complete genome sequence of XaF13, a novel bacteriophage of *Xanthomonas vesicatoria* from México. *Microbiol. Resour. Announc.* **2020**, *9*, e01371-19. [CrossRef]
22. Yamamoto, K.R.; Alberts, B.M.; Benzinger, R.; Lawhorne, L.; Treiber, G. Rapid bacteriophage sedimentation in the presence of polyethylene glycol and its application to large-scale virus purification. *Virology* **1970**, *40*, 734–744. [CrossRef]
23. Ríos-Sandoval, M.; Quiñones-Aguilar, E.E.; Solís-Sánchez, G.A.; Enríquez-Vara, J.N.; Rincón-Enríquez, G. Complete genome sequence of *Xanthomonas vesicatoria* bacteriophage ΦXaF18, a contribution to the biocontrol of bacterial spot of pepper in México. *Microbiol. Resour. Announc.* **2020**, *9*, e00213-20. [CrossRef]
24. Di Rienzo, J.; Balzarini, M.; Gonzalez, L.; Tablada, E.; Casanoves, F.; Robledo, C. *InfoStat*, version 2008; Grupo InfoStat, FCA, Universidad Nacional de Córdoba: Córdoba, Argentina, 2008.
25. Bonenfant, Q.; Noe, L.; Touzet, H. Porechop ABI: Discovering unknown adapters in oxford nanopore technology sequencing reads for downstream trimming. *Bioinform. Adv.* **2023**, *3*, vbac085. [CrossRef]

26. Kolmogorov, M.; Yuan, J.; Lin, Y.; Pevzner, P.A. Assembly of long, error-prone reads using repeat graphs. *Nat. Biotechnol.* **2019**, *37*, 540–546. [CrossRef]
27. Antipov, D.; Korobeynikov, A.; McLean, J.S.; Pevzner, P.A. HybridSPAdes: An algorithm for hybrid assembly of short and long reads. *Bioinformatics* **2016**, *32*, 1009–1015. [CrossRef] [PubMed]
28. Prjibelski, A.; Antipov, D.; Meleshko, D.; Lapidus, A.; Korobeynikov, A. Using SPAdes *de novo* assembler. *Curr. Protoc. Bioinform.* **2020**, *70*, e102. [CrossRef]
29. Li, H. Minimap2: Pairwise alignment for nucleotide sequences. *Bioinformatics* **2018**, *34*, 3094–3100. [CrossRef]
30. Okonechnikov, K.; Golosova, O.; Fursov, M. Unipro UGENE: A unified bioinformatics toolkit. *Bioinformatics* **2012**, *28*, 1166–1167. [CrossRef]
31. Moraru, C.; Varsani, A.; Kropinski, A.M. VIRIDIC—A novel tool to calculate the intergenomic similarities of prokaryote-infecting viruses. *Viruses* **2020**, *12*, 1268. [CrossRef] [PubMed]
32. Kumar, S.; Stecher, G.; Suleski, M.; Sanderford, M.; Sharma, S.; Tamura, K. MEGA12: Molecular evolutionary genetic analysis version 12 for adaptive and green computing. *Mol. Biol. Evol.* **2024**, *41*, msae263. [CrossRef] [PubMed]
33. Sullivan, M.J.; Petty, N.K.; Beatson, S.A. Easyfig: A genome comparison visualizer. *Bioinformatics* **2011**, *27*, 1009–1010. [CrossRef]
34. Zanotti, G.; Grinzato, A. Structure of filamentous viruses. *Curr. Opin. Virol.* **2021**, *51*, 25–33. [CrossRef]
35. Lefkowitz, E.J.; Dempsey, D.M.; Hendrickson, R.C.; Orton, R.J.; Siddell, S.G.; Smith, D.B. Virus taxonomy: The database of the International Committee on Taxonomy of Viruses (ICTV). *Nucleic Acids Res.* **2018**, *46*, D708–D717. [CrossRef]
36. Tom, E.F.; Molineux, I.J.; Paff, M.L.; Bull, J.J. Experimental evolution of uv resistance in a phage. *PeerJ* **2018**, *6*, e5190. [CrossRef]
37. Born, Y.; Bosshard, L.; Duffy, B.; Loessner, M.J.; Fieseler, L. Protection of *Erwinia amylovora* bacteriophage Y2 from UV-induced damage by natural compounds. *Bacteriophage* **2015**, *5*, e1074330. [CrossRef]
38. Jo, S.J.; Kim, S.G.; Park, J.; Lee, Y.M.; Giri, S.S.; Lee, S.B.; Jung, W.J.; Hwang, M.H.; Park, J.H.; Roh, E.; et al. Optimizing the formulation of *Erwinia* bacteriophages for improved uv stability and adsorption on apple leaves. *Heliyon* **2023**, *9*, e22034. [CrossRef] [PubMed]
39. Gašić, K.; Kuzmanović, N.; Ivanović, M.; Prokić, A.; Šević, M.; Obradović, A. Complete genome of the *Xanthomonas euvesicatoria* specific bacteriophage KΦ1, its survival and potential in control of pepper bacterial spot. *Front. Microbiol.* **2018**, *9*, 2021. [CrossRef] [PubMed]
40. Ikehara, K. Isolation of a clear plaque-forming mutant of *Escherichia coli* or infectivity assay of filamentous phage Fd. *Virology* **1974**, *62*, 570–572. [CrossRef] [PubMed]
41. Kuo, T.-T.; Chiang, C.-C.; Chen, S.-Y.; Lin, J.-H.; Kuo, J.-L. A long lytic cycle in filamentous Phage Cf1tv infecting *Xanthomonas campestris* pv. citri. *Arch. Virol.* **1994**, *135*, 253–264. [CrossRef]
42. Kuo, M.-Y.; Yang, M.-K.; Chen, W.-P.; Kuo, T.-T. High-frequency interconversion of turbid and clear plaque strains of bacteriophage F1 and associated host cell death. *Can. J. Microbiol.* **2000**, *46*, 841–847. [CrossRef]
43. Shieh, G.-J.; Charng, Y.-C.; Yang, B.-C.; Tu, J.; Bau, H.-J.; Kuo, T.-T. Identification and nucleotide sequence analysis of an open reading frame involved in high-frequency conversion of turbid to clear plaque mutants of filamentous phage Cf1t. *Virology* **1991**, *185*, 316–322. [CrossRef]
44. Koonin, E.V. The second cholera toxin, Zot, and Its plasmid-encoded and phage-encoded homologues constitute a group of putative ATPases with an altered purine NTP-binding motif. *FEBS Lett.* **1992**, *312*, 3–6. [CrossRef] [PubMed]
45. Mai-Prochnow, A.; Hui, J.G.K.; Kjelleberg, S.; Rakonjac, J.; McDougald, D.; Rice, S.A. Big things in small packages: The genetics of filamentous phage and effects on fitness of their host. *FEMS Microbiol. Rev.* **2015**, *39*, 465–487. [CrossRef] [PubMed]
46. Stefani, E.; Obradović, A.; Gašić, K.; Altin, I.; Nagy, I.K.; Kovács, T. Bacteriophage-mediated control of phytopathogenic xanthomonads: A promising green solution for the future. *Microorganisms* **2021**, *9*, 1056. [CrossRef]
47. Di Pierro, M.; Lu, R.; Uzzau, S.; Wang, W.; Margaretten, K.; Pazzani, C.; Maimone, F.; Fasano, A. Zonula occludens toxin structure-function analysis: Identification of the fragment biologically active on tight junctions and of the zonulin receptor binding domain. *J. Biol. Chem.* **2001**, *276*, 19160–19165. [CrossRef]
48. Benyamini, P. Phylogenetic tracing of evolutionarily conserved Zonula occludens toxin reveals a "high value" vaccine candidate specific for treating multi-strain *Pseudomonas aeruginosa* infections. *Toxins* **2024**, *16*, 271. [CrossRef] [PubMed]
49. Iribarren, C.; Plaza, N.; Ramírez-Araya, S.; Pérez-Reytor, D.; Urrutia, Í.M.; Suffredini, E.; Vicenza, T.; Ulloa, S.; Fernández, J.; Navarrete, P.; et al. Presence of Zonula occludens toxin-coding genes among *Vibrio Parahaemolyticus* isolates of clinical and environmental origin. *Microorganisms* **2024**, *12*, 504. [CrossRef]

50. Roux, S.; Krupovic, M.; Daly, R.A.; Borges, A.L.; Nayfach, S.; Schulz, F.; Sharrar, A.; Matheus Carnevali, P.B.; Cheng, J.-F.; Ivanova, N.N.; et al. Cryptic *Inoviruses* revealed as pervasive in bacteria and archaea across earth's biomes. *Nat. Microbiol.* **2019**, *4*, 1895–1906. [CrossRef]
51. Hopkins, M.; Kailasan, S.; Cohen, A.; Roux, S.; Tucker, K.P.; Shevenell, A.; Agbandje-Mckenna, M.; Breitbart, M. Diversity of environmental single-stranded DNA phages revealed by PCR amplification of the partial major capsid protein. *ISME J.* **2014**, *8*, 2093–2103. [CrossRef]

Disclaimer/Publisher's Note: The statements, opinions and data contained in all publications are solely those of the individual author(s) and contributor(s) and not of MDPI and/or the editor(s). MDPI and/or the editor(s) disclaim responsibility for any injury to people or property resulting from any ideas, methods, instructions or products referred to in the content.